

Application of Continues Wavelet Transform to Investigate the Resolution Effect of Digital Elevation Model on Topographic Index Distribution

Vahid Nourani

Abstract— Current progress in computer, geographic information system (GIS) and remote sensing technology has led to the LIDAR (light detection and ranging) data, as a new generation of high-resolution digital elevation model (DEM). Although such a high resolution DEM can be a useful tool for terrain analysis, high amount of noise is also expected to be existent in a mega-data set. To deal with this problem in this study, continues wavelet transform (CWT), as a mathematical filter, was employed to extract slope, specific area and topographic index which are important parameters in hydro-environmental studies at different resolutions. In this way the proposed methodology was applied to 1-m resolution LIDAR DEM of the Elder Creek River watershed where is a sub-basin of the South Folk Eel River basin at California. The results were also compared favorably with the results of a classic method. The result indicates that smoothing ability of the wavelet can be a promising DEM processing alternative to cope with the noise and pits of a high resolution DEM.

Index Terms— DEM, Elder Creek River, GIS, LIDAR Topography, Wavelet transform.

I. INTRODUCTION

To apply some hydro-environmental models, the spatial distribution of the so-called topographic index (TI) is calculated for the catchment from a topographic data set, such as a digital elevation model (DEM). The basic and most common form of the topographic index, $\ln(a/\tan \beta)$, is the natural logarithm of the ratio of the cumulative upslope area per unit contour length (specific catchment area), a to the local slope of the ground surface, $\tan \beta$.

The evolution of affordable, robust computers and commonplaceness of geographical information system (GIS) are encouraging the use of different GIS-based terrain algorithms to calculate the primary topographic characteristics of ' $\tan \beta$ ' and ' a ' which are then combined to form the secondary topographic characteristic of the TI. O'Callaghan and Mark [1] introduced the D8 (eight flow directions) method as the earliest and simplest algorithm for specifying flow direction and accumulation area. Thereafter,

some other methods such as multiple flow direction (MFD, [23]), modified MFD [3], infinite possible flow directions (D_∞) [4] and hybrid MFD- D_∞ [5] have also been suggested as attempts to overcome the limitation of D8 method. On the other side, finite difference, linear regression and quadratic equation methods have been employed for calculating local ground surface slope ($\tan \beta$) from DEMs [6]. There are also a number of studies which compare the patterns of TI computed in different ways (e.g., [7]). However, a recurring scale issue regarding TI is that the distribution of TI is markedly related to the topographic information content of the DEM, which can be impacted by both discretization (or aggregation) and smoothing effects [8]. Several studies have discussed the effects of scale and DEM resolution on the TI distribution (e.g., [3], [8]–[14]). Also, the recent emergence of airborne altimetry technology (e.g., light detection and ranging, LIDAR) as a means of acquiring high resolution DEMs, allows the examination of this scale issue using much finer grid cell size (see, [15]).

Beyond the shadow of a doubt, the scale dependence of TI distribution effects on the model's parameters and performance. In the case of using coarser DEMs, it has been postulated that a positive shift accompanied, sometimes by a deformation may be appeared in the TI distribution and although the calibration of parameters can often compensate for the lack of resolution, the physical interpretation of the parameters and the merit of the model in distributed predictions may be lost [10], [16]. On the other hand, some other problems may have arisen if very high resolutions DEMs are employed. Zhang and Montgomery [14] stated that increasing the resolution to 2 or 4 m would not provide important additional information and often 10 m cell size is sufficient for hydrologic simulation to have a compromise between accuracy and computation cost in large area. Cai and Wang [17] found that a 90 m DEM can derive TI distribution as well as a 30 m DEM for landscapes with significant variation in elevation; but Sorensen and Seibert [15] utilized high resolution LIDAR data to show the large influence of the DEM's information content meanwhile, simply going from a 5 to 10-m resolution can considerably affect the calculated TI. Beven *et al.* [18] describe required resolution as needing to be fine enough to reflect the effect of topography;

Manuscript Received July 09, 2011.

Vahid Nourani, Associate Prof., Dept. of Water Resources Eng., Faculty of Civil Eng., Univ. of Tabriz, Tabriz, Iran; Formerly, Visiting Associate Prof., St. Anthony Falls Lab. and NCED, Dept. of Civil Eng., Univ. of Minnesota, USA, Phone No. +98-411-339-2409, Mobile No. +98-914-403-0332. (e-mail: vnourani@yahoo.com; vnourani@umn.edu).

Application of continues wavelet transform to investigate the resolution effect of digital elevation model on topographic index distribution

too coarse a DEM may fail to represent convergent slope features and results in parameter inconsistency across scales, while too fine a DEM may impose perturbation to the flow directions and slope angles. Furthermore, as the resolution of topographic data is fined, like any other signal, there is a greater possibility that the DEM includes artificial depressions and pits which result from random noise [19]. Aforementioned studies bear out that even the implementation of high-resolution DEMs which are becoming more readily available nowadays, does not warrant the improvement of the modeling if a modification or/and DEM pre-processing is not taken into consideration. In this way, the wavelet transform as such a DEM pre-processing tool may be incorporated into a GIS framework for the de-noising and compression purposes [20].

In this study, the capability of the wavelet transform which has recently found wide application in geophysics [21], topographic feature extraction [19], [22], [23] and hydrological simulation [24]–[26] is examined as an alternative for DEM and TI processing computed from a high-resolution LIDAR DEM.

II. STUDY AREA

The study area which is the subject of this research is the Elder Creek sub-basin of the South Fork Eel River in northern California, USA (Fig. 1). This 16.84 km² basin drains a landscape of steep hill slopes and narrow canyons. The length of its main channel is about 8 km with an average stream gradient of 80 m/km. The texturally-filtered DEM of the Elder Creek Basin was extracted from 1.0 m LIDAR DEM of the South Fork Eel River watershed which is a part of University of California at Berkley’s NCALM (National Center for Airborne Laser Mapping) project and can be retrieved via (www.ncalm.org) (Fig. 2).

III. WAVELET TRANSFORM

The one dimensional (1-D) wavelet transform of a continuous signal, $f(x)$, is defined as [27]:

$$d_w(a_w, b_w) = \frac{1}{\sqrt{a_w}} \int_{-\infty}^{+\infty} \psi^* \left(\frac{x - b_w}{a_w} \right) f(x) dx \quad (1)$$

Where ψ^* corresponds to the complex conjugate and $\psi(x)$ is

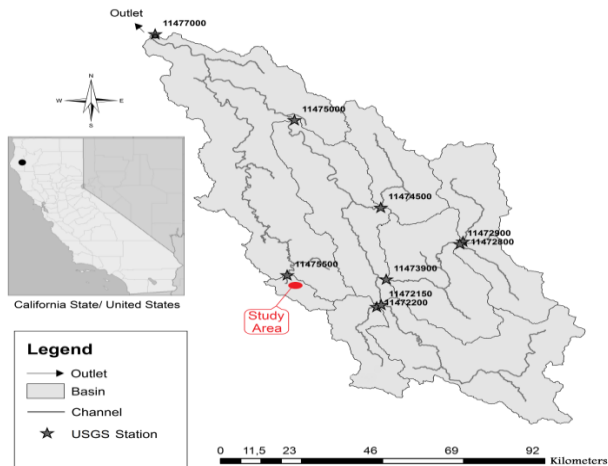


Fig. 1 Eel River map and study area location

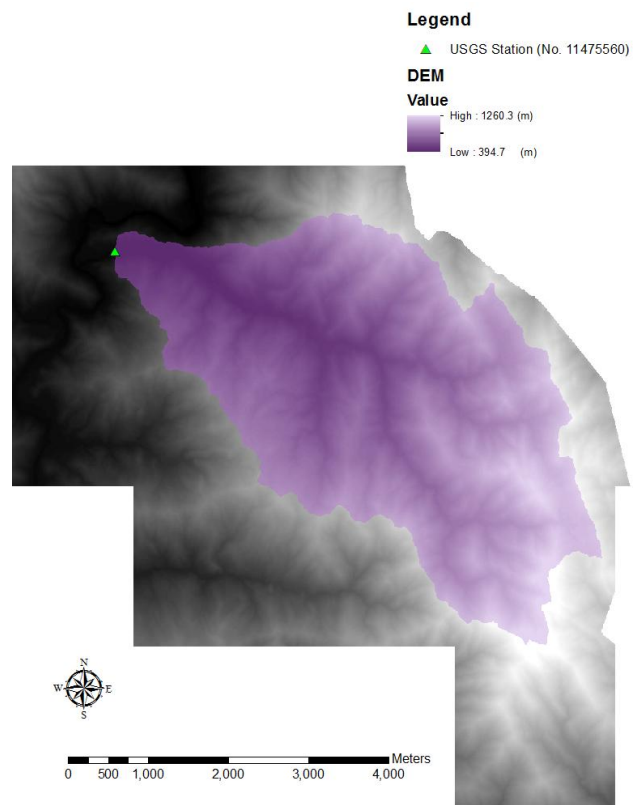


Fig. 2 Study area DEM

called wavelet function or mother wavelet. The parameter a_w acts as a dilation factor, while b_w corresponds to a temporal or spatial translation of the function $\psi(x)$, which allows the study of the signal around b_w . In order to be classified as a wavelet, a function must have finite energy, and it must satisfy the following "admissibility conditions" [27]:

$$\int_{-\infty}^{+\infty} \psi(x) dx = 0, \quad C_\psi = \int_{-\infty}^{+\infty} \frac{|\hat{\psi}(w)|^2}{|w|} dw < \infty \quad (2)$$

where, $\hat{\psi}(w)$ is Fourier transform of $\psi(x)$; i.e., the wavelet must have no zero frequency component. In order to obtain a reconstruction formula for the studied signal, it is necessary to add "regularity condition" to the previous ones [27]:

$$\int_{-\infty}^{+\infty} x^l \psi(x) dx = 0 \quad \text{Where } l = 1, 2, \dots, k-1 \quad (3)$$

So the original signal may be reconstructed using the inverse wavelet transform as [27]:

$$f(x) = \frac{1}{C_\psi} \int_{-\infty}^{+\infty} \int_0^{\infty} \frac{1}{\sqrt{a_w}} \psi \left(\frac{x - b_w}{a_w} \right) d_w(a_w, b_w) \frac{da_w db_w}{a_w^2} \quad (4)$$

Almost all of the algorithms for specifying flow direction and specific area including D8 and D ∞ , use first order finite difference method to compute local slope. This method magnifies the DEM’s noise since it considers a sudden jump and discontinuity, as a step function, between the elevations of two adjacent cells. Thus, a smoothing filter may be utilized to reduce the noise effect when high-resolution DEM is used to compute the local slopes. In the context of channel network extraction, Lashermes *et al.* [22] applied convolution product with the kernel ‘g’ on the elevation height (h) as:



$$\frac{\partial(h * g)}{\partial x} = \frac{\partial h}{\partial x} * g = h * \frac{\partial g}{\partial x} \quad (5)$$

$$\text{in which } (h * g)_{(x)} = \int_0^x h(t) g_{(x-t)} dt$$

to compute the smoothed slope via the continuous wavelet transform (CWT).

Comparison of (5) with (1) implies that slope in x-direction smoothed by the kernel 'g', i.e. $m_x = \frac{\partial h}{\partial x} * g$, is equal to the wavelet coefficient of DEM with mother wavelet of $\frac{\partial g}{\partial x}$. Similarly, m_y and then magnitude and direction of steepest slope are computed for each cell as:

$$m = \sqrt{m_x^2 + m_y^2} \quad (6)$$

and,

$$\tan \beta = \gamma \pi + \arctan\left(\frac{m_y}{m_x}\right) \quad (7)$$

Where, $\gamma=0$ if $m_x > 0$; $\gamma=1$ if $m_x < 0$ and $m_y > 0$; $\gamma=-1$ if $m_x < 0$ and $m_y < 0$. Thereafter, computed slope can be used to calculate specific upslope area and TI distribution. In this study, the first derivative of the Gaussian function as the Gaussian wavelet with unit energy, in the form of (8) was applied to the 1-m resolution DEM in both x and y directions to compute magnitude and direction of slope and then spatial distribution of TI were extracted.

$$\frac{\partial g}{\partial x} = \left(\frac{32}{\pi}\right)^{\frac{1}{4}} x e^{-x^2} \quad (8)$$

The Gaussian wavelet is popular in geophysical applications, particularly in terrain analysis because its shape, as shown in Fig. 3, is similar to the topography form. It is worthy of note that the wavelet transform should be applied to an extended area started from outside of the study's region in order to cope with the edge effect [28].

IV. RESULTS AND DISCUSSION

The NCLAM's 1-m resolution LIDAR DEM was re-sampled into 2, 4, 8, 16, 32 and 60-m resolution DEMs. Instead of using the localized mean which may lead to an overly smoothed topography, the aggregation process was performed by passing the aggregation window of target size across the original 1-m resolution DEM and assigning the elevation of the central pixel of window to the corresponding pixel in the coarser DEM. For the re-sampled DEMs the classic sink removal method [29] was applied and TI distributions were computed using the most common flow pathway algorithm (i.e., D8) and also CWT methods. The results have been presented in Figs. (4a) and (4b) for D8 and CWT methods, respectively which indicate that by increasing the grid cell size, not only a positive shift in mean of TI distribution is appeared but also higher order

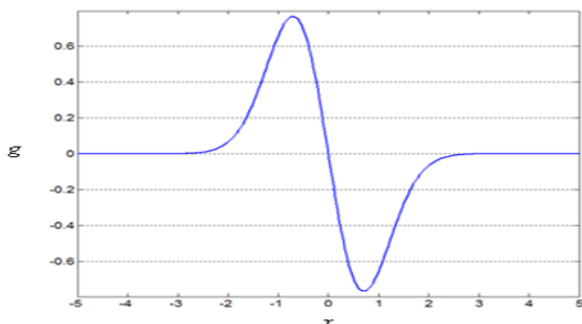


Fig. 3 Gaussian wavelet

momentums of the distribution may also be changed. Finer grid sizes typically lead to larger values of $\tan \beta$ and smaller values of a since steeper hill slopes and smaller drainage area are resolved and as a result provide smaller TI values. Fig. 5 compares calculated TI distributions by two algorithms using 1- and 32-m resolution DEMs. In CWT method, the calculated local slope is smaller than computed slope by D8. Therefore, the discrepancy between two distributions is more marked especially in the beginning of the distribution which grid sizes typically lead to larger values of $\tan \beta$ and smaller values of a since steeper hill slopes and smaller drainage area are resolved and as a result provide smaller TI values. Fig. 5 compares calculated TI distributions by two algorithms using 1- and 32-m resolution DEMs. In CWT method, the calculated local slope is smaller than computed slope by D8. Therefore, the discrepancy between two distributions is more marked especially in the beginning of the distribution which his related to steep headwaters and more sensitive to the cell size. However in the coarser grid size, the whole trend of the flow pathway is almost identical in both methods. Of course, the magnitude of the discrepancy depends on the catchment's terrain and as an evidence for the importance of slope; the TI distribution is more sensitive to the grid size and flow direction algorithm for the steeper catchments such as Elder Creek Basin.

Also, according to Figs.(6a)and (6b) which show respectively the spatial distributions of TI within the basin extracted from 1 and 8-m resolution DEMs, for the finer DEM the structure of the TI distribution is much complex and irregular. In addition to the slope, the specific area may also cause this complexity. The smallest value of the specific area equals to the grid cell size and in a low resolution DEM, a cell in a down slope valley position will have a large specific area value. However, the cells in the similar positions of the corresponding high resolution DEM may have either a large specific area if they are located along the channel or a small specific area if they have slightly higher elevation than the surrounding cells and located outside of the channel.

A large number of TIs with low and even negative values can be seen in the computed distribution by 1-m resolution DEM (see Fig.6a). According to the fractal property of the topography there is an exponential relationship between the elevation difference (Δh) and distance (ϵ) of two adjacent cells within the basin's DEM as [30], [6]:

$$\Delta h = \alpha \epsilon^{2-D} \rightarrow \tan \beta = \frac{\Delta h}{\epsilon} = \alpha \epsilon^{1-D} \quad (9)$$

Since the fractal dimension (D) and proportionality coefficient (α) are constant for the topography, by decreasing the grid cell size (ϵ) the local slope is increased. Furthermore, it has been already shown that the uncertainly in slope has a grid spacing dependence and as grid is fined, there is a greater probability of error in slope [31]. Consequently, it is clear that in a high-resolution DEM, the high slopes result in very low (even negative) values of TI on steep slopes. The complexity of the local slope ($\tan \beta$) distribution, extracted from 1-m resolution DEM, at different parts of the basin may lead to this outcome (Fig. 7).

Application of continues wavelet transform to investigate the resolution effect of digital elevation model on topographic index distribution

Similar result and argument were reported by Quinn *et al.* [3] and Lane *et al.* [32] using 5 and 2-m resolution DEMs, respectively. Quinn *et al.* [3] reasoned that this is because fining DEM resolution tends to increase the numbers of cells with a low specific area value whilst leaving the overall slope gradient the same. Also as it was previously mentioned, the fractal theory which implies the scale effect on the local slope value and also the noise and pits are other important reasons for the phenomenon. In spite of DEM and slope smoothing potential of applied CWT, some negative TI values (about 0.7%) can be still seen in Fig. (6a). Two arguments are conceivable for such performance of the CWT. The first is related to the basis geometry, so that at very steep slope or cliff having a shape like the step function, the filtering may even yield to much larger slope values. The second is that the applied CWT just acts on x and y directions without any filtering across diagonal direction wherever may need to be smoothed.

The effect of change in TI distribution may be imposed to the hydro-environmental model. Although the change in the TI distribution is offset by calibration of the model's parameter(s) to match the simulated and observed hydrographs, such re-optimized parameters may lead to unreasonable results when tested against internal field data [3].

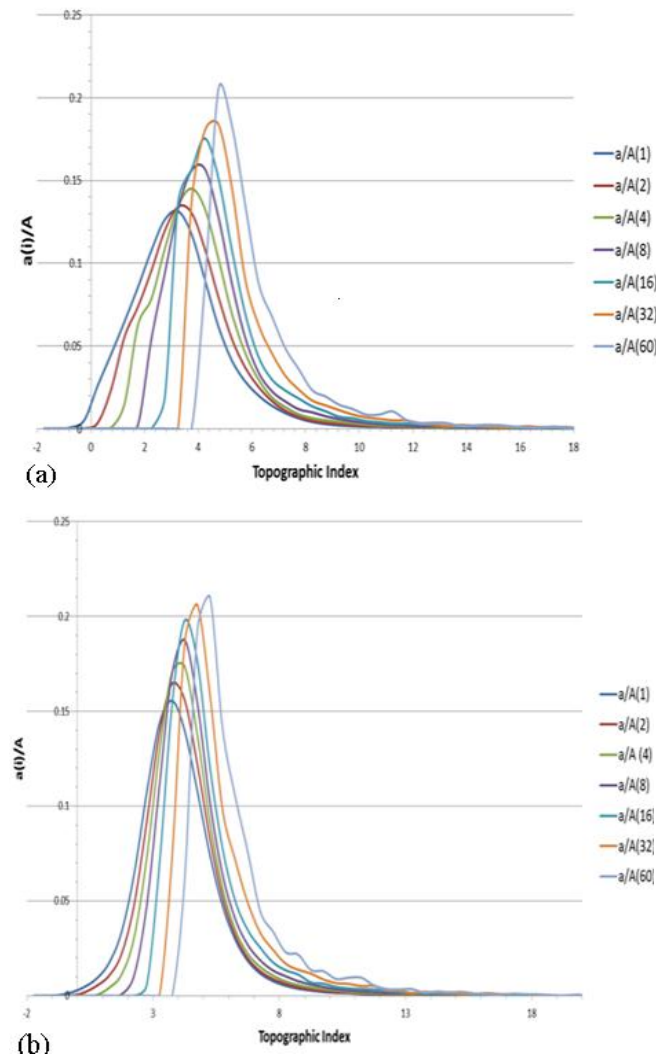


Fig. 4 Computed TI distributions by a) D8 b) CWT methods
Therefore, considering the developments in new generation of high resolution DEM, it may become apparent that the

application of finer grid resolution is more appropriate to the observed processes.

However as mentioned formerly, some other problems may be faced when a high-resolution DEM is used; such as corruption of the terrain analysis by error in terms of instrument noise or scale irregularities in general [31], [22], and [19].

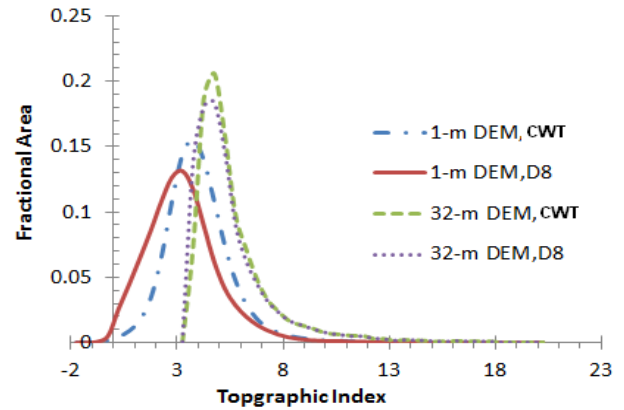


Fig. 5 Comparison of calculated TI distributions by two algorithms using 1- and 32-m resolution DEMs.

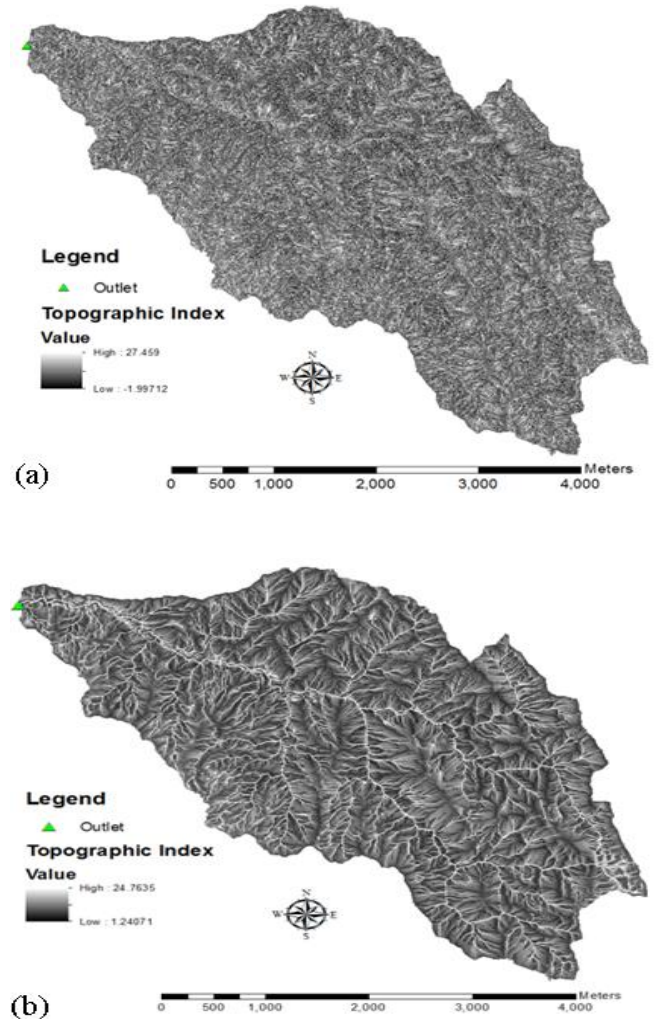


Fig. 6 Spatial distribution of TI extracted from DEM with resolution a) 1-m, b) 8-m

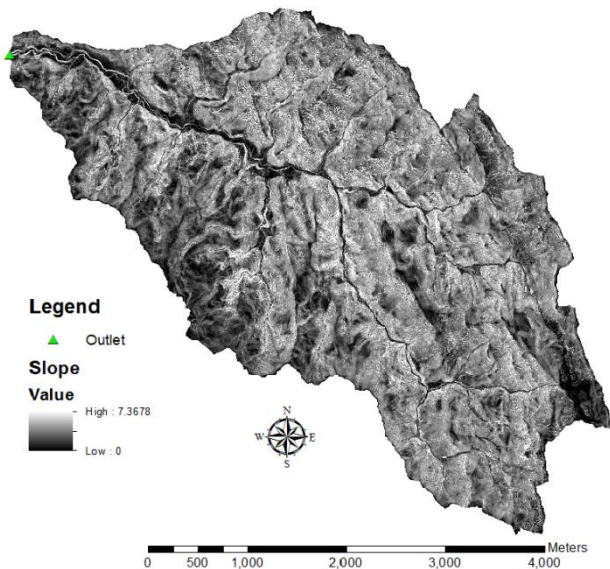


Fig. 7 Spatial distribution of the slope extracted from original 1-m resolution DEM

V. CONCLUSION

In this study, the concept of continuous wavelet transform (CWT) was used to compute local ground surface slope and then cumulative drainage area and topographic index (TI) distribution of the watershed which are important geomorphologic parameters in the hydro-environmental studies. The Gaussian CWT was applied to the DEMs at different resolutions extracted from the high-resolution LIDAR DEM. A systematic trend could be seen in the computed TI distributions at different resolutions; so that by decreasing the resolution of the DEM, the mean of the distribution is increased. Furthermore, there is a discrepancy between the mean and formation of the computed distributions by the classic D8 and proposed CWD methods. The smoothing ability of the CWT allows to the method to handle the existing pits and noise in the high-resolution DEM.

It is recommended to employ the wavelet-based TI distribution in a hydro-environmental model and verify its ability in a real world problem. A few studies have been already presented to downscale the TI distribution from a coarse-resolution DEM and in most of them by neglecting the scale effect on the slope value, it has been assumed that TI distribution at different scales have similar shapes but not necessarily similar means (e.g., [33], [34]). However as a research plan for the future study, the fractal (or multi-fractal) concept and proposed wavelet analysis may be conjugated and used for downscaling and re-scaling of the TI distribution.

REFERENCES

1. J.F. O'Callaghan, and D.M. Mark, "The extraction of drainage networks from digital elevation data", *Comput. Vis. Graph. Im. Proc.*, Vol.28, 1984, pp. 28–344.
2. P.F. Quinn, K.J. Beven, P. Chevallier, and O. Planchon, "The prediction of hill slope flow paths for distributed modeling using digital terrain models", *Hydrol. Process.*, Vol.5, 1991, pp.59–80.
3. P.F. Quinn, K.J. Beven, and R. Lamb, "The $\ln(a/\tan\beta)$ index: How to calculate it and how to use it within the TOPMODEL framework", *Hydrol. Process.*, Vol.9, 1995, pp.161–182.

4. D.G. Tarboton, "A new method for the determination of flow directions and upslope areas in grid digital elevation models", *Water Resour. Res.*, Vol.33, No.2, 1997, pp.309–319.
5. J. Seibert, and B.L. McGlynn, "A new triangular multiple flow direction algorithm for computing upslope areas from gridded digital elevation models", *Water Resour. Res.*, Vol.43, 2007, 04501, doi:10.1029/2006WR005128.
6. X. Zhang, N.A. Drake, J. Wainwright, and M. Mulligan, "Comparison of slope estimates from low resolution DEMs: scaling issues and a fractal method for their solution", *Earth Surf. Proc. Land.*, Vol.24, 1999, pp.763–779.
7. R. Sorensen, U. Zinko, and J. Seibert, "On the calculation of the topographic wetness index: evaluation of different methods based on field observations", *Hydrol. Earth Syst. Sc.*, Vol.10, 2006, pp.101–112.
8. D.M. Wolock, and C.V. Price, "Effects of digital elevation model map scale and data resolution on a topography-based watershed model", *Water Resour. Res.*, Vol.30, 1994, pp. 3041–3052.
9. P. Bruneau, C. Gascuel-Oudou, P. Robin, P. M'erot, and K. Beven, "Sensitivity to space and time resolution of a hydrological model using digital elevation data", *Hydrol. Process.*, Vol.9, 1995, pp.69–81.
10. M. Franchini, J. Wendling, C. Obled, and E. Todini, "Physical interpretation and sensitivity analysis of the TOPMODEL", *J. Hydrol.*, Vol.175, 1996, pp.293–338.
11. G.R. Hancock, "The use of digital elevation models in the identification and characterization of catchments over different grid scales", *Hydrol. Process.*, Vol.19, No.9, 2005, 1727–1749.
12. G. Mendicino, and A. Sole, "The information content theory for the estimation of the topographic index distribution used in TOPMODEL", *Hydrol. Process.*, Vol.11, 1997, pp.1099–1114.
13. G-M. Saulnier, K. Beven, and C. Obled, "Digital elevation analysis for distributed hydrological modelling: reducing scale dependence in effective hydraulic conductivity values", *Water Resour. Res.*, Vol.33, 1997, pp.2097–2101.
14. W. Zhang, and D.R. Montgomery, "Digital elevation model grid size, landscape representation, and hydrologic simulations", *Water Resour. Res.*, Vol.30, 1994, pp.1019–1028.
15. R., Sorensen, and J. Seibert, "Effects of DEM resolution on the calculation of topographical indices: TWI and its components", *J. Hydrol.*, Vol.347, 2007, pp.79–89.
16. V. Nourani, and A. Mano, "Semi-distributed flood runoff model at the sub-continental scale for south-western Iran", *Hydrol. Process.*, Vol.21, 2007, pp. 3173–3180.
17. X. Cai, and D. Wang, "Spatial autocorrelation of topographic index in catchments", *J. Hydrol.*, Vol.328, No.3–4, 2006, pp.581–591.
18. K.J. Beven, R. Lamb, P.F. Quinn, R. Romanowicz, and J. Freer, "TOPMODEL. In Computer Models of Watershed Hydrology", Singh V.P. (ed.), Water Resource Publications, Colorado, 1995.
19. P. Passalacqua, P. Tarolli, and E. Foufoula-Georgiou, "Testing space-scale methodologies for automatic geomorphic feature extraction from LIDAR in a complex mountainous landscape", *Water Resour. Res.*, Vol.46, 2010, W11535.
20. J. T. Bjorke, and S. Nilsen, "Wavelets applied to simplification of digital terrain models", *Int. J. Geogr. Inf. Sci.*, Vol.17, No.7, 2003, pp.601-621.
21. E. Foufoula-Georgiou, and P. Kumar, *Wavelet in Geophysics*, Academic Press, New York 1995.
22. B. Lashermes, E. Foufoula- Georgiou, and W. E. Dietrich, "Channel network extraction from high resolution topography using wavelets", *Geophys. Res. Lett.*, Vol.34, 2007, L23S04.
23. D., Wang, and X. Cai, "Scale and resolution effects of topographic index by 2-D continuous wavelet transform", *Proc. Int. Conf. Flood Forecasting Water Resour. Assess.*, 2006, Beijing, China.
24. D. Labat, "Recent advances in wavelet analyses: part 1–A review of concepts", *J. Hydrol.*, Vol.314, 2005, pp.275–288.
25. V. Nourani, M.T. Alami, and M.H. Aminfar, "A combined neural-wavelet model for prediction of Ligvanchai watershed precipitation", *Eng. Appl. Artif. Intell.*, Vol.22, 2009a, pp.466–472.
26. V., Nourani, M. Komasi, and A. Mano, "A multivariate ANN-wavelet approach for rainfall-runoff modeling", *Water Resour. Manag.*, Vol.23, No.14, 2009b, pp.2877–2894.
27. S.G. Mallat, *A Wavelet Tour of Signal Processing*. Second Edition. Academic Press, San Diego, 1998.
28. P. S. Addison, *The Illustrated Wavelet Transform Hand-Book*, Institute of Physics Publishing, London, 2002.

Application of continues wavelet transform to investigate the resolution effect of digital elevation model on topographic index distribution

29. V. Nourani, V.P. Singh, and H. Delafrouz, "Three geomorphological rainfall– runoff models based on the linear reservoir concept", *Catena*, Vol.76, No.3, 2009c, pp.206–214.
30. N.R. Pradhan, Y. Tachikawa, and K. Takara, "A downscaling method of topographic index distribution for matching the scales of model application and parameter identification", *Hydrol. Process.*, Vol.20, 2006, pp.1385–1405.
31. S.N. Lane, R.M. Westaway, and D.M. Hicks, "Estimation of erosion and deposition volumes in a large gravel-bed, braided river using synoptic remote sensing", *Earth Surf. Proc. Land.*, Vol.28, 2003, pp.249–271.
32. S.N. Lane, C.J. Brookes, M.J. Kirkby, and J. Holden, "A network index based version of TOPMODEL for use with high resolution digital topographic data", *Hydrol. Process.*, Vol.18, 2004, pp.191–201.
33. R. Ibbitt, and R. Woods, "Re-scaling the topographic index to improve the representation of physical processes in catchment models", *J. Hydrol.*, Vol.293, 2004, pp.205–218.
34. D.M. Wolock, and G.J. McCabe, "Differences in topographic characteristics computed from 100- and 1000-m resolution digital elevation model data", *Hydrol. Process.*, Vo.14, No.6, 2000, pp.987–1002.

AUTHORS PROFILE



Vahid Nourani was born in Tabriz, Iran in 1975 and received his B.Sc. and M.S. degrees in Civil Engineering from University of Tabriz, Iran in 1998 and 2000, respectively. He then continued his graduate study in Civil and Environmental Engineering in the field of Hydrology at Shiraz University, Iran and Tohoku University, Japan and was graduated in 2005. Nourani was with the Faculty of Civil Engineering, University of Tabriz as an Assistant Professor from 2005-2009 and as Associate Professor from 2009-2010 and in this period, 34 Ph.D. and M.Sc. students were graduated under his technical supervision. Currently, he is a visiting Associate Professor in St. Anthony Falls Laboratory of Civil Engineering Department at University of Minnesota, USA. His research interests include rainfall-runoff modeling, Artificial Intelligence in water resources engineering, Hydroinformatics and computational hydraulics. His researches outcomes have been published as 32 Journal articles, 2 book chapters and more than 40 papers presented in international and national conferences. He is currently researching about 2-D wavelet transform applications in hydrological simulation.